Structure-Based Design of Inhibitors Specific for Bacterial Thymidylate Synthase[†,‡]

Thomas J. Stout,[§,||] Donatella Tondi,[⊥,#] Marcella Rinaldi,[#] Daniela Barlocco,[#] P. Pecorari,[#] Daniel V. Santi,[@] Irwin D. Kuntz,[@] Robert M. Stroud,*[,§] Brian K. Shoichet,*[,⊥] and M. Paola Costi*[,#]

Departments of Biochemistry and Biophysics, University of California, San Francisco, California 94143-0448, Department of Molecular Pharmacology & Biological Chemistry, Drug Discovery Program, Northwestern University Medical School, 303 East Chicago Avenue, Chicago, Illinois 60611-3008, Department of Pharmaceutical Chemistry, University of California, San Francisco, California 94143-0448, and Dipartimento di Scienze Farmaceutiche, Universita di Modena, Via Campi 183, 41100 Modena, Italy

Received July 6, 1998; Revised Manuscript Received November 19, 1998

ABSTRACT: Thymidylate synthase is an attractive target for antiproliferative drug design because of its key role in the synthesis of DNA. As such, the enzyme has been widely targeted for anticancer applications. In principle, TS should also be a good target for drugs used to fight infectious disease. In practice, TS is highly conserved across species, and it has proven to be difficult to develop inhibitors that are selective for microbial TS enzymes over the human enzyme. Using the structure of TS from *Lactobacillus casei* in complex with the nonsubstrate analogue phenolphthalein, inhibitors were designed to take advantage of features of the bacterial enzyme that differ from those of the human enzyme. Upon synthesis and testing, these inhibitors were found to be up to 40-fold selective for the bacterial enzyme over the human enzyme. The crystal structures of two of these inhibitors in complex with TS suggested the design of further compounds. Subsequent synthesis and testing showed that these second-round compounds inhibit the bacterial enzyme at sub-micromolar concentrations, while the human enzyme was not inhibited at detectable levels (selectivities of 100−1000-fold or greater). Although these inhibitors share chemical similarities, X-ray crystal structures reveal that the analogues bind to the enzyme in substantially different orientations. Site-directed mutagenesis experiments suggest that the individual inhibitors may adopt multiple configurations in their complexes with TS.

Thymidylate synthase (TS)[1] is an attractive target for the design of drugs used against proliferative diseases because of its central role in the production of DNA. TS catalyzes the methylation of 2′-deoxyuridine 5′-monophosphate (dUMP) by N^5,N^{10}-methylene tetrahydrofolate (CH_2H_4folate). This reaction is the terminal step in the only de novo synthetic pathway to thymidylate, which is essential for DNA production. Inhibition of TS stops the production of DNA, disrupting the progression through the cell cycle and eventually leading to "thymineless" cell death (*1*).

Much effort in drug design against TS has focused on inhibitors that resemble the substrate, dUMP, or the cofactor, CH_2H_4folate. A mechanism-based inhibitor of TS (*2*), 5-fluorouridylate, which is administered as the premetabolite, 5-fluorouracil (5-FU), is used in chemotherapy. The TS inhibitor, 10-propargyl-5,8-dideazafolate (CB3717), is a mimic of the cofactor, CH_2H_4folate (*3*). Although CB3717 is a potent inhibitor of TS [K_i of 40 nM (*4*)], it shows liver and kidney toxicity in a small number of patients (*5*). Recent structure-based drug design efforts against TS (*6*−*11*, *41*, *42*) have resulted in a series of potent compounds such as AG337 and Tomudex that bind in the folate binding site of the enzyme. These new compounds show promise as cancer chemotherapeutics.

The amino acid sequence of TS is highly conserved across species, particularly among those residues that form the substrate and cofactor binding pockets (*12*). These residues also interact closely with inhibitors such as 5-fluorouridylate,

[†] Portions of this work were supported by starter and faculty development grants from the PhRMA foundation and by the Howard Hughes Medical Institute through a faculty development grant to Northwestern University (to B.K.S.), by a MURST grant and by the CIGS and CICAIA (to M.P.C.), and by the National Institutes of Health (Grants GM24485 and CA-41323 to R.M.S., Grant GM31497 to I.D.K., and Grant CA14394 to D.V.S.). D.T. was partly supported by a doctoral fellowship from Dipartimento di Scienze Farmaceutiche, Università di Modena. T.J.S. was supported by a postdoctoral fellowship from the American Cancer Society.

[‡] Coordinates for the complexes of LcTS with compounds **4** and **5** have been deposited with the Brookhaven Protein Data Bank under entry codes 1TSL and 1TSM, respectively.

* Corresponding authors. E-mail: stroud@msg.ucsf.edu (R.M.S.), b-shoichet@nwu.edu (B.K.S.), and costimp@unimo.it (M.P.C.).

[§] Departments of Biochemistry and Biophysics, University of California.

[||] Current address: *Meta*Xen, 280 E. Grand Ave., South San Francisco, CA 94080.

[⊥] Northwestern University Medical School.

[#] Universita di Modena.

[@] Department of Pharmaceutical Chemistry, University of California.

[1] Abbreviations: TS, thymidylate synthase; dUMP, 2′-deoxyuridine monophosphate; CH_2H_4folate, N^5,N^{10}-methylene tetrahydrofolate; dTMP, 2′-deoxythymidine monophosphate; 5-FU, 5-fluorouracil; CB3717, 10-propargyl-5,8-dideazafolate; EcTS, *Escherichia coli* thymidylate synthase; LcTS, *Lactobacillus casei* thymidylate synthase; HTS, *Homo sapiens* (human) thymidylate synthase; **1**, phenolphthalein; **2**, diphenol-2,3-naphthalein; **3**, diphenol-1,8-naphthalein; **4**, 3′,3″-dichlorophenol-1,8-naphthalein; **5**, diphenol-5-nitro-1,8-naphthalein; **6**, 3′,3″-dichlorophenolphthalein; **7**, 3′,3″-dichlorophenol-4-chloro-1,8-naphthalein; **8**, 3′-chlorophenol-4-nitro-1,8-naphthalein; DMSO, dimethyl sulfoxide; MR, molecular replacement; F_o, observed structure factor; F_c, calculated structure factor; α_{calc}, phases derived from the atomic coordinates.

10.1021/bi9815896 CCC: $18.00
Published on Web 01/13/1999

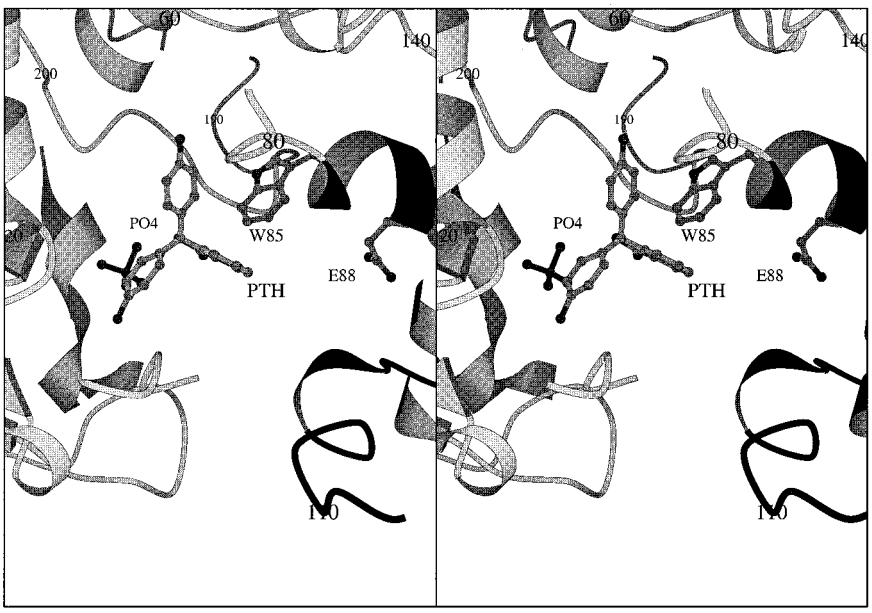

FIGURE 1: Crystal structure of phenolphthalein (PTH) bound to TS from *L. casei* (*14*). Every tenth C_α is labeled, and the bacterial "small domain" insertion (residues 90−139) is dark gray. This figure were prepared using the program BOBSCRIPT (R. Esnouf, 1996, unpublished).

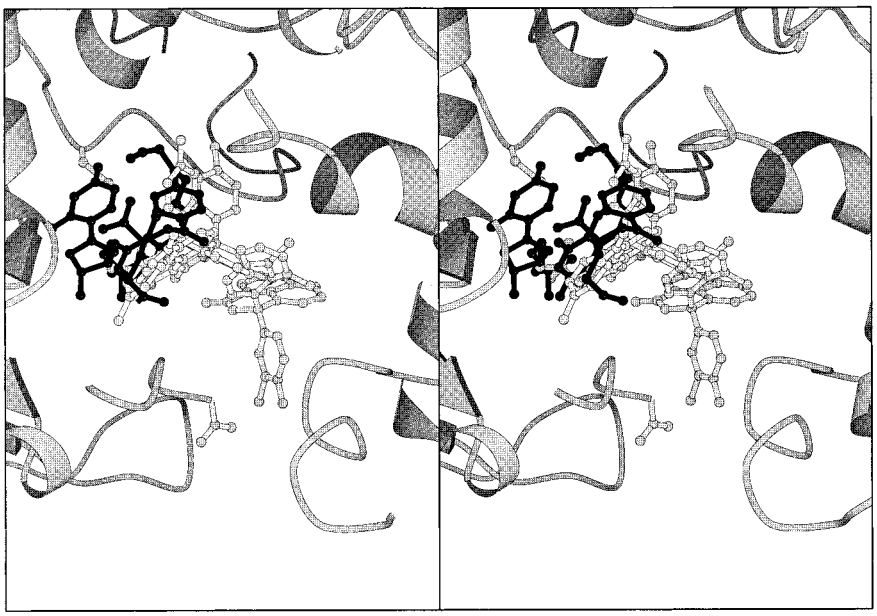

FIGURE 2: Superposition of the crystal structures of each of the complexes discussed [LcTS−phenolphthalein, −**4**, and −**5** (all in white ball-and-stick representations) with the complex of LcTS with substrate, dUMP, and cofactor analogue, CB3717 (PDB entry 1LCA), which are both drawn as black stick representations]. Note that the crystallographic binding modes of these species-specific inhibitors are all well removed from the substrate binding pocket. This figure were prepared using the program BOBSCRIPT (R. Esnouf, 1996, unpublished).

CB3717, BW1843U89, Tomudex, and AG337. Folate binding site inhibitors such as CB3717, ZD1694 (Tomudex), and BW1843U89 are broadly cytotoxic to dividing cells, and show little selectivity for microbial versus human TS (HTS) (*13*). Thus, these compounds are not candidates for antimicrobial chemotherapy. Given the recent rise in antibiotic resistance, novel drug candidates in this area would be welcome.

The marked conservation of the substrate-binding region of TS among organisms suggests that species-specific inhibitor discovery should target nonsubstrate regions of the binding site. We have previously described an inhibitor of TS, phenolphthalein (**1**), whose binding site (Figure 1) is displaced from that of the substrate (Figure 2) (*14*). The phenolphthalein binding site borders on residues of the *Lactobacillus casei* TS (LcTS) that belong to an insertion unique to certain bacterial forms of TS. This insertion, referred to as the "small domain", spans residues 90−139 in LcTS (Figure 1). Several of these residues are conserved among TS enzymes from microbial pathogens, such as *Streptomyces aureas* (*15*). Although phenolphthalein itself is not selective for bacterial versus human TS, we reasoned that analogues of phenolphthalein that took advantage of this region in *L. casei* would be selective for this and similar enzymes over the human enzyme.

Here we describe the design and testing of derivatives of phenolphthalein meant to be specific for LcTS versus HTS. In designing these new derivatives, we sought to take

Table 1: Specificities and Inhibition Constants for Phthalein Analogues

Compound	Structure	K_i LcTS (μM)	IC_{50} LcTS	K_i HTS (μM)	IC_{50} HTS	Specificity[a, b]
phenolphthalein	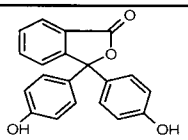	4.7	12	0.35	1.2	0.1
2	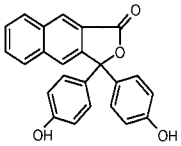	7.0	20	—	—	—
3	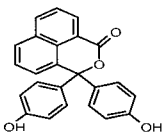	2.8	27	19.7	67	2.5
4	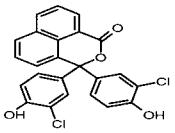	0.7	1.3	30.3	52	40
5	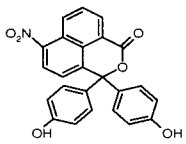	1.0	9.7	5.0	18.2	1.9
6	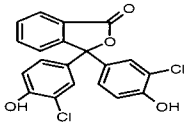	1.9	23	0.7	3	0.1
7	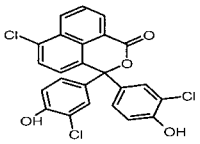	0.73	4.2	—	>> 64[c]	>100[d]
8	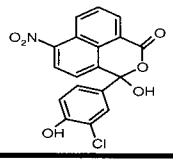	0.25	0.26	—	>>200[c]	>> 1000[d]

[a] Specificity measured as IC_{50}(LcTS)/IC_{50}(HTS). [b] Specificity measured as K_i(LcTS)/K_i(HTS). [c] No inhibition measured at this concentration, close to the solubility limit of the compound. [d] Assuming ≤10% inhibition at the solubility limit.

advantage of regions of LcTS, proximal to the phenolphthalein binding site, that are not present in HTS. Upon synthesis and testing, the most specific derivative had a 40-fold selectivity for LcTS versus HTS. Crystallographic studies of a specific and a nonspecific analogue showed that these compounds bound in different orientations to LcTS, suggesting a mechanism for the differential specificities. Using this information, new analogues were designed, synthesized, and tested. These second-round compounds were both more potent and more selective than the initial derivatives, with sub-micromolar affinities for the bacterial enzyme but with the affinity for the human enzyme essentially eliminated. Several of these inhibitors showed specific toxicity for bacteria such as *S. aureas* versus human cells in in vitro studies (*16*). These inhibitors are candidates for further elaboration as antimicrobial chemotherapeutics.

EXPERIMENTAL PROCEDURES

Inhibitor Design. Phenolphthalein (**1**) analogues **2**−**4** were designed to complement the small domain region of LcTS (residues 90−139), based on visual inspection of the complex between phenolphthalein (**1**) and LcTS (Figure 1) (*14*).

As a model for HTS, we used the structure of TS from *Escherichia coli* (*17*). Although the HTS structure has been determined, the structure is thought to reflect an inactive form of the enzyme in which a large portion of the active site is rearranged into an architecture which makes the binding of and enzymatic activity on substrates unlikely (*18*). The *E. coli* TS crystal structure has been used successfully as a model of the human enzyme in previous inhibitor design studies (*6*−*11*, *41*, *42*). The identities of the *E. coli* residues at positions 82, 83, and 264 were changed to those of the human residues by graphical modeling. Thus, Glu82 was truncated to alanine, Trp83 modified to asparagine, and Ile264 modified to valine. The human residue was overlapped onto the corresponding *E. coli* atom positions; for the Trp83 to asparagine substitution, the N_δ of the asparagine was modeled to overlap with the N_ϵ of Trp. No close contacts were introduced by these modeled substitutions. For comparison of compounds **1**, **4**, and **5** in the LcTS versus putative

HTS complexes, the structure of the "humanized" EcTS was rms-fit onto the LcTS structure using the main chain C_α atoms. In evaluating the fit of **5** in the humanized EcTS structure, we used the conformation of Trp85 adopted in the LcTS−**5** complex.

Chemistry. The synthetic scheme for the various derivatives is described in detail in an accompanying paper (*16*). Briefly, the phthalein and naphthalein derivatives were prepared through reaction of the anhydride precursor of the phthalein ring system with the appropriate phenolic derivative. A mixture of the appropriate anhydride (0.01 mol) and phenolic derivative (0.02 mol) and a few drops of concentrated H_2SO_4 was heated while it was being stirred at 180 °C for 5 h. After cooling, the residue was purified by silica gel chromatography eluting with dichloromethane/methanol (95/5) to give as the first run the unreacted anhydride followed by the desired product. Stock solutions of each of the compounds were prepared in dimethyl sulfoxide (DMSO) and stored at −20 °C until they were used. The molar extinction coefficients of all compounds were measured in DMSO solution at a concentration of approximately 10^{-4} M.

Enzymology. LcTS and HTS were expressed and purified as described previously (*19*−*21*); the enzymes were greater than 95% homogeneous as determined by SDS−PAGE. Purified enzyme was stored at −80 °C in 10 mM phosphate buffer (pH 7.0) and 0.1 mM EDTA until it was used. Enzymatic assays were carried out with a Perkin-Elmer UV lamba 16 spectrophotometer equipped with a multicell system and thermoregulated with a Haake F3C circulating bath. The activity of the enzymes was determined spectrophotometrically by following the increasing absorbance at 340 nm due to the oxidation reaction of CH_2H_4folate to dihydrofolate (*4*). In these activity assays, (6*R*,*S*)-CH_2H_4folate was used at a concentration of 180 μM, dUMP at 120 μM, and enzyme at 0.07 μM. Enzyme kinetic experiments were conducted under standard conditions (*22*): 50 mM TES buffer (pH 7.4), 75 mM β-mercaptoethanol, 25 mM $MgCl_2$, 6.5 mM formaldehyde, and 1 mM EDTA. In all cases, unless otherwise noted, the enzyme concentration was 0.07 μM, and the substrate (dUMP) concentration was 120 μM. The CH_2H_4folate concentration was 60 μM for IC_{50} calculations and was varied for K_i calculations. We note that the K_m values of HTS and of LcTS for folate are similar: 8 and 10 μM, respectively. Thus, comparing the IC_{50} (or K_i) values for the two enzymes gives a good indication of specificity. Inhibitors were delivered from the DMSO stocks to the buffered solution. Reactions were initiated by the addition of enzyme. For assays with mutant LcTS enzymes, previously expressed and purified mutant enzymes were used, as described previously (*2*, *23*−*25*).

X-ray Crystallography. Since compounds **4** and **5** have low aqueous solubilities, saturated solutions were prepared in DMSO. Complex crystals were grown with the addition of 1 μL of a ligand solution to a 10 μL hanging drop containing 9 μL of 6 mg/mL LcTS, 1 μL of 10% ammonium sulfate, and 1 mM DTT, and inverted over wells containing 20 mM KPO_4 (pH 6.8) and 1 mM DTT. Rapid precipitation of the ligands was seen on addition of the DMSO solution to the crystallization experiment. Crystals began growing within this precipitate in 2−4 days. Control drops containing only apo-LcTS began to crystallize in 1−2 days. Crystal growth continued for 4−5 days. Control crystals grew to a maximum of 800 μm, but complex crystals grew to no larger than 450 μm in the principle (c^*) dimension. Complex crystals, like apo-LcTS, are hexagonal bipyramids, but distinctly orange in color due to the presence of the highly colored inhibitors. The crystals belong to space group $P6_1$22 with the following unit cell dimensions: $a = 78.3$ Å and $c = 243.2$ Å. The crystallographic asymmetric unit contains one LcTS monomer.

Table 2: X-ray Diffraction Data and Refinement Statistics

parameter	LcTS−**4**	LcTS−**5**
a (Å)	78.3	78.3
c (Å)	243.2	243.2
γ (deg)	120.0	120.0
space group	$P6_122$	$P6_122$
maximum resolution (Å)	2.5	3.0
no. of measured reflections	78644	35352
no. of observed reflections[a]	29742	16758
no. of unique reflections	9477	7727
completeness[a] (%)	58.7	80.0
R_{symm} (%)	8.12	12.4
average redundancy	3.8	4.6
refinement resolution (Å)	8−2.5	8−3.0
refined R_{factor}	0.163	0.175
R_{free}	0.251	0.222
no. of modeled waters	313	247
rms bonds (Å)	0.006	0.012
rms angles (deg)	1.4	1.9
rms dihedrals (deg)	23.7	24.6
rms impropers (deg)	1.08	1.45
G-factor[b]	0.28	0.13

[a] $I/\sigma(I) \geq 2.0$. [b] The G-factor is a measure of the overall "normality" of the structure. The overall G-factor reported by PROCHECK (*27*) was obtained from an average of all the different G-factors for each residue in the structure.

X-ray diffraction data from a 200 μm × 200 μm × 450 μm crystal of the LcTS−**4** complex were collected on an R-Axis IIc imaging plate with a Rigaku RU-200 rotating anode generator operating at 15 kW (50 mA and 300 kV) and equipped with a Cu anode ($\lambda = 1.5418$ Å). The crystal to detector distance was 230 mm, and the detector was set at −15° in 2θ. Exposures of 20 min per 1° of oscillation range were used throughout the data collection. The diffraction data were indexed, integrated, scaled, and merged to 2.5 Å resolution with the R-Axis software from MSC (Table 2). A total of 78 644 observations were integrated, scaled, and merged, yielding 9477 unique reflections [60% complete with $F > 2\sigma(F)$] between 48.6 and 2.5 Å [$R_{symm}(I) = 0.081$ with an average redundancy of 3.8].

X-ray diffraction data from a 125 μm × 125 μm × 300 μm crystal of the LcTS−**5** complex were collected using the same equipment and settings. Exposures of 30 min per 1° of oscillation range were used. The data were indexed, integrated, scaled, and merged to 3.0 Å resolution using the HKL software package (*26*) (Table 2). A total of 35 352 observations were integrated, scaled, and merged, yielding 7727 unique reflections between 50.0 and 3.0 Å. The data were 80% complete with $F \geq 2\sigma(F)$; $R_{symm}(I)$ equaled 0.124 with an average redundancy of 4.6.

Since both complexes crystallized in a lattice isomorphous with the unliganded form of the enzyme, initial difference electron density Fourier syntheses ($F_o - F_c$) were calculated using the refined coordinates for apo-LcTS without ordered waters or counterion. The initial difference density for

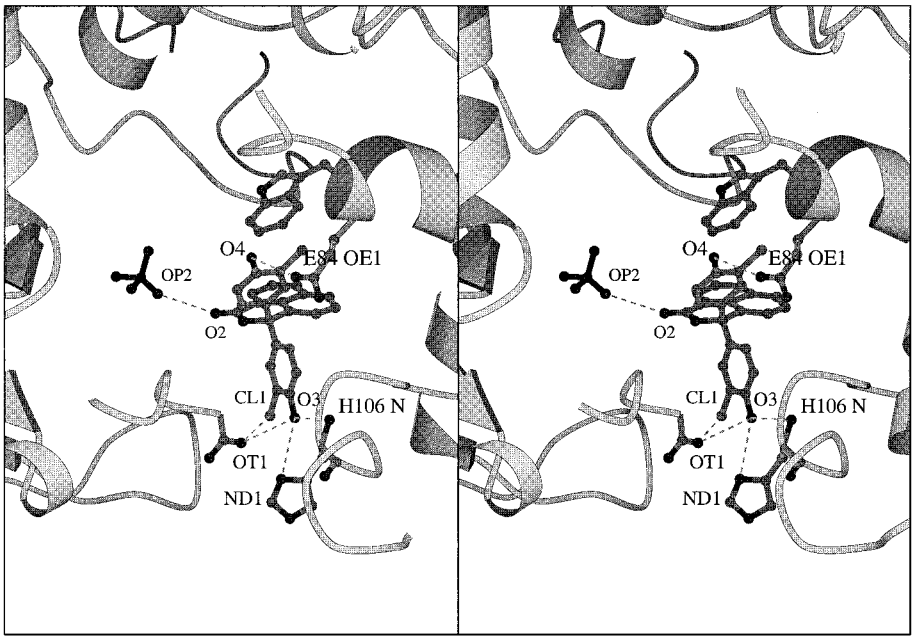

FIGURE 3: Crystal structure of compound **4** bound to *L. casei* TS. Important protein−ligand interactions (see the text) are labeled and indicated with dashed lines. This figure were prepared using the program BOBSCRIPT (R. Esnouf, 1996, unpublished).

compound **4** was roughly spherical in shape when contoured at 3σ. It was not possible to uniquely orient compound **4** into this density. Since least-squares refinement procedures modify the working model to account for all features of the crystallographic data possible, features that are not currently represented in the model can be refined away through global accommodation of the model. In this case, detailed features of the binding mode of **4** were found by applying a random positional displacement (a "shake") to all atoms of the protein model that varied as a Gaussian distribution between 0 and 0.1 Å in magnitude. The protein was not yet refined against the diffraction data obtained for this complex. A difference Fourier synthesis was calculated using the "shaken" model and is displayed in Figure 4a. This map clearly shows a bilobal distribution of the electron density projecting from the original difference density. The two phenol moieties could now be modeled into these lobes and the naphthalein ring into the larger portion of the difference density. Subsequent refinement clarified the positions of the *m*-chlorine substituents as shown in a final simulated annealing omit map (Figure 4b), calculated after the protein had been refined against the data, but from which the ligand (**4**) has been omitted.

The initial difference electron density map ($F_o - F_c$) for the LcTS−**5** complex was devoid of significant features above 2.5σ. However, the strong coloration of the crystals suggested that significant amounts of the ligand had been incorporated into the crystal lattice. Therefore, the more sensitive ΔF_o calculation was used to locate any possible reduced occupancy binding sites. This calculation uses the difference between the observed diffraction amplitudes {-[F_{obs}(apo) − F_{obs}(complex)]α(apo)} from two closely related data sets (here, apo-LcTS and the LcTS−**5** complex) rather than the difference between the amplitudes for the structure of interest and calculated amplitudes based on the current model {[F_{obs}(complex) − F_{calc}(complex)]α(complex)}. The resulting Fourier synthesis reveals only those features which differ between the two crystal structures. The additional sensitivity of this calculation enabled us to observe the location and orientation of **5**, as well as any differences in the protein structure relative to the apo structure. On the basis of this calculation, we were able to place and successfully refine a model of compound **5** in the complex structure (Figure 5).

RESULTS

Four analogues of phenolphthalein (**1**) were initially synthesized and tested for activity as inhibitors of LcTS and HTS: diphenol-2,3-naphthalein (**2**), diphenol-1,8-naphthalein (**3**), 3′,3″-dichlorophenol-1,8-naphthalein (**4**), and 5-nitrodiphenol-1,8-naphthalein (**5**). Phenolphthalein was not specific for LcTS versus HTS, inhibiting the human enzyme more potently than the bacterial enzyme rather than the reverse (IC_{50} values of 1.2 μM for HTS and 12 μM for LcTS; specificity ratio of 0.1). Conversely, the new inhibitors were more specific for the bacterial enzyme (Table 1). This was especially true of compound **4**, which had a specificity ratio of 40 and a K_i of 0.7 μM against LcTS. A fifth analogue, the 3′,3″-dichloro derivative of phenolphthalein (**6**), was then synthesized to test a mechanism for possible specificity (see the Discussion).

X-ray Crystal Structures. The LcTS−**4** complex was elucidated by difference Fourier techniques to 2.5 Å resolution and refined to an R_{factor} of 0.163 (R_{free} = 0.251) using X-PLOR (*28*). The final model consists of well-modeled positions for all 316 amino acids in one monomer of LcTS, 315 well-ordered solvent molecules, one phosphate ion in the dUMP binding site, and one modeled binding orientation of compound **4**. The refined coordinates for the LcTS−**4** complex have been deposited with the Brookhaven Protein Data Bank as entry 1TSL.

The LcTS−**5** complex was determined by difference Fourier techniques to 3.0 Å resolution and refined to an R_{factor} of 0.175 (R_{free} = 0.222) using X-PLOR (*28*). The final model

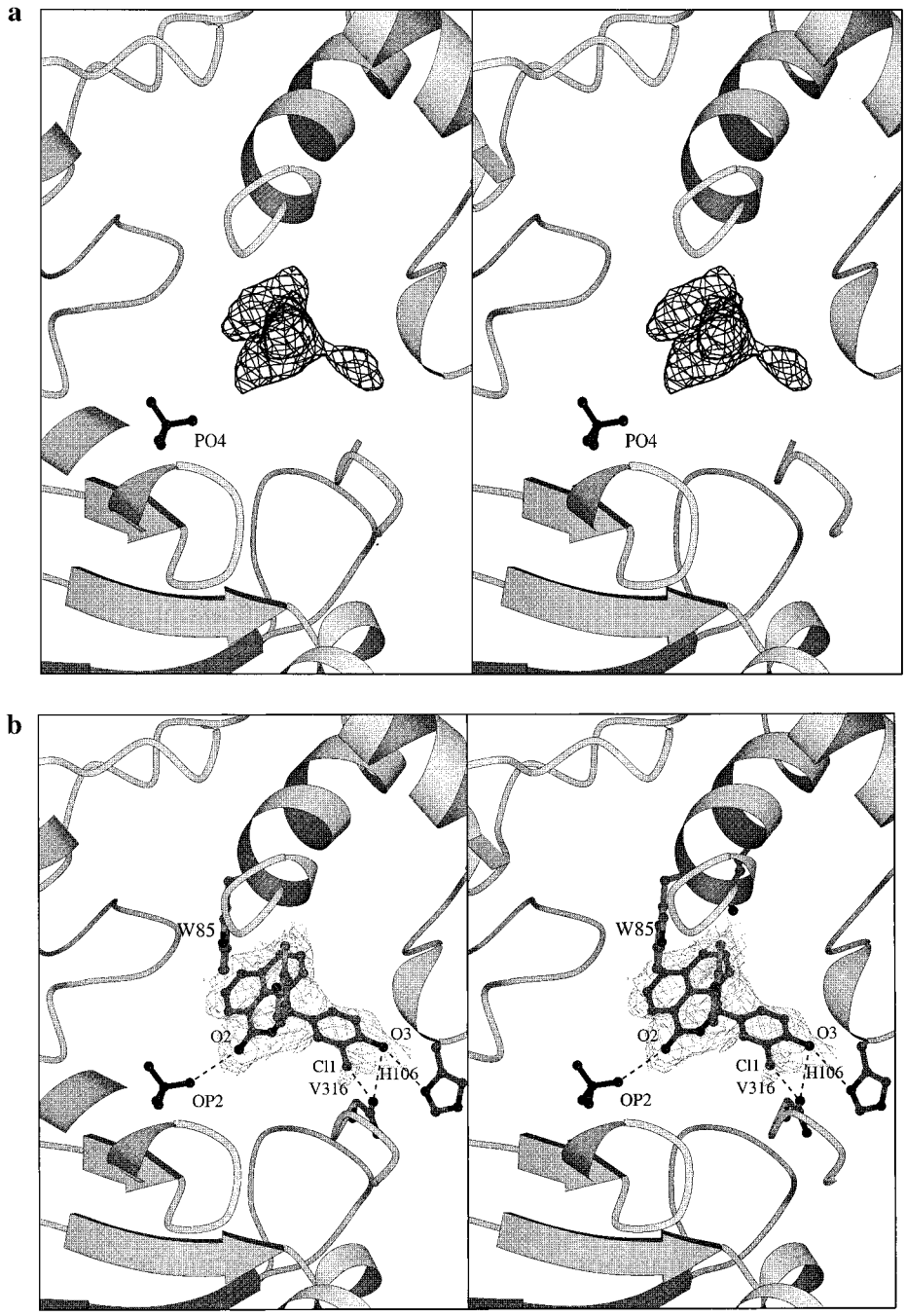

FIGURE 4: (a) Initial difference map (Fourier coefficient map of $F_o - F_c$, contoured at 3σ) of the TS active site. No refinement of the protein against the diffraction data has been done, and compound **4** has not yet been modeled into this density. (b) Simulated annealing "omit" map showing difference electron density ($F_o - F_c$, contoured at 3σ) for compound **4** in the *L. casei* TS. This calculation uses all of the atoms of the structure except those of the ligand and is unbiased by refinement with inclusion of the ligand molecule. This figure were prepared using the program BOBSCRIPT (R. Esnouf, 1996, unpublished).

consists of well-modeled positions for all 316 amino acids in one monomer of LcTS, 247 well-ordered solvent molecules, one phosphate ion in the dUMP binding site, and one modeled binding orientation of compound **5**. We note that the number of solvent molecules in both complexes is high for structures at such resolutions. However, the protein model is based on a good quality structure determined to 2.3 Å resolution with excellent geometry (PDB entry 4TMS). Thus, the model phases are effectively at higher resolution and lower mean error than a de novo structure determined at this resolution, giving us greater confidence in the positions of ordered water molecules than would normally be the case. The refined coordinates for the LcTS−**5** complex have been deposited with the Brookhaven Protein Data Bank as entry 1TSM.

Further Inhibitors. Compound **7**, the 4-chloro derivative of **4**, was synthesized to take advantage of specificity opportunities observed in the LcTS−**4** complex. This derivative was a mixed type inhibitor (*29*) of LcTS with a K_i value of 0.7 μM. The compound had no detectable affinity for HTS (Table 1). Several monophenolic derivatives were also synthesized (*16*) to explore possible steric restriction imposed by the diphenolic substitutions, but in general, these compounds showed low activity. An exception was compound

Table 3: Contacts Observed between LcTS and Phenolphthalein, **4**, and **5**[a]

inhibitor	atom	contact distance (Å)	LcTS residue	LcTS atom	HTS residue
phenolphthalein	phenol 1 OH	2.6	water 404	O	NA[b]
phenolphthalein	phenol 1 OH	3.3	Glu60	$O_\epsilon1$	Glu
phenolphthalein	C_{16}	4.7	Trp82	$C_\delta2$	Trp
phenolphthalein	C_9	3.8	Trp85	$N_\epsilon1$	Trp
phenolphthalein	phthalein O	2.7	Trp85	$C_\zeta2$	Asn
phenolphthalein	phthalein O	3.9	Arg23	$N_\eta2$	Arg
phenolphthalein	phthalein O	3.6	water 363	O	NA[b]
phenolphthalein	phenol 2 OH	2.3	Asp221	$O_\delta1$	Asp
phenolphthalein	phenol 2 C_{18}	2.9	Val314	$C_\delta1$	Met
phenolphthalein	phenol 2 C_{20}	4.7	Val316	$C_\delta1$	Val
phenolphthalein	phenol 2 C_{20}	3.4	Glu84	C_γ	Ala
4	naphthalein O_2[c]	3.4	phosphate	O	phosphate
4	naphthalein O_2[c]	3.0	water 361	O	NA[b]
4	naphthalein C_2	4.6	Trp85	$C_\zeta3$	Asn
4	naphthalein C_2	4.6	Trp85	CH2	Asn
4	naphthalein C_4	4.6	Ala194	C_α	Ala
4	naphthalein C_7	3.3	Glu88	$O_\epsilon1$	Arg
4	naphthalein C_8	3.1	Glu88	$O_\epsilon2$	Arg
4	phenol Cl_1	3.7	Thr24	$C_\gamma2$	Thr
4	phenol O_3[c]	3.1	Val316	OT	Val
4	phenol C_{16}	3.7	Val316	C_β	Val
4	phenol O_3[c]	3.4	His106	$N_\delta1$	NA[b]
4	phenol O_3[c]	3.4	His106	N	NA[b]
4	phenol O_3[c]	2.7	water 627	O	NA[b]
4	water 627	2.8	Asp103	$O_\delta2$	NA[b]
4	phenol O_4[c]	2.9	Glu84	O_ϵ[1]	Ala
4	phenol Cl_2	3.0	Glu84	C_β	Ala
4	phenol C_{21}	3.4	Trp85	$C_\zeta2$	Asn
4	phenol Cl	3.5	Trp85	$C_\delta2$	Asn
4	phenol C_{20}	3.6	Trp85	$C_\eta2$	Asn
5	naphthalein O_2[d]	2.8	water 357	O	NA[b]
5	water 357	3.0	Arg23	N_ϵ	Arg
5	naphthalein O_2[d]	3.4	phosphate	O	phosphate
5	naphthalein C_4	3.6	Asp221	$O_\delta2$	Asp
5	phenol 1 C_{16}	3.5	Leu195	$C_\delta2$	Leu
5	phenol 1 C_{17}	3.7	Leu195	C_β	Leu
5	phenol 1 O_3[d]	2.5	Trp82	$C_\zeta3$	Trp
5	phenol 1 C_{17}	3.2	Trp85	$C_\epsilon3$	Asn
5	phenol 2 O_4[d]	3.2	Glu88	$O_\epsilon1$	Arg
5	phenol 2 C_{23}	3.1	Glu84	C_β	Ala
5	phenol 2 C_{24}	4.1	Glu84	C_γ	Ala

[a] Also indicated is the corresponding residue in human TS. [b] Not appropriate because water is absent or the residue is missing. [c] See Figure 3. [d] See Figure 6.

Table 4: Effect of Mutant Residues on Apparent Inhibition Constants

ligand	binding constant (μM)[a]			
	wild type	V316A	W82Y	E60D
CH_2H_4folate	10	370	10	36.8
phenolphthalein	4.7	15	2.0	1.6
3	2.8	11	−	NI[b]
4	0.7	13	1	4.4
5	1.0	13	−	0.4

[a] The values reported for CH_2H_4folate are K_m values, and the values for the inhibitors are K_i values. [b] No inhibition measured at 30 μM inhibitor.

8, which had a K_i value of 0.25 μM and specificities over the human enzyme of >1000-fold (Table 1).

Mutant Studies. The effect on inhibitor binding to several site-directed mutant TS enzymes was also tested (Table 4). The compounds tested included phenolphthalein and compounds **3**−**5**. The mutant enzymes were E60D (*23*), W82Y (*12*), and V316A. These substitutions typically diminished the extent of inhibitor binding by 3−20-fold; several substitutions improved the extent of inhibitor binding by up to 2.5-fold.

DISCUSSION

This study was initiated with the crystal structure of the phenolphthalein−TS complex (*14*). Visual inspection suggested that analogues of phenolphthalein with larger functional groups extending from the phthalein ring system would complement residues specific to certain bacterial forms of TS, including LcTS, which were not present in the human enzyme. These included residues Glu84, Trp85, Glu88, and the "small domain" (residues 90−139) of LcTS (Figure 1).

Initial Inhibitor Design. Compounds **2**−**5** were synthesized to test this hypothesis. The most selective of the new inhibitors was compound **4**, which was 40-fold more selective for LcTS compared to HTS, and had a 6-fold higher affinity than phenolphthalein (Table 1). The differential selectivity of compound **4** compared to compounds **3** and **5** was unexpected (**4** has a selectivity index of 40, compound **3** has a selectivity index of 2.5, and **5** has a selectivity index of 1.8). Compound **4** differs from **3** and **5** in the presence of *o*-chlorine substitutions on the phenolic rings, and the possibility that the haloderivatization of the phenolic rings formed the basis of specificity was considered.

To address this question, the 3′,3″-dichloro derivative of phenolphthalein (**6**) was synthesized. The specificity ratio for compound **6** was found to be 0.13 (i.e., it inhibited HTS better than LcTS, rather than the reverse), similar to that found for phenolphthalein. This suggested that the specificity advantage of compound **4** is a convolution of the effects of the chlorine and naphthalide derivatizations, though perhaps the naphthalide extension had a greater effect. Although the initial hypothesis had led to the desired increase in specificity, it was clear that the reasons for the specificity increase were more complicated than anticipated.

*X-ray Crystal Structures of LcTS in Complex with **4** and **5***. To address the molecular basis of specificity, the structure of **4** bound to LcTS was determined by X-ray crystallography. The 2.5 Å resolution structure of this complex showed **4** making interactions with LcTS that differed considerably from those made by phenolphthalein (Figures 3 and 7). Rather than the naphthalide moiety extending into the small domain from the phenolphthalein anchor position, as had been designed, compound **4** was displaced from the phenolphthalein binding site by approximately 5 Å. The phenolic O_3 hydroxyl (Figure 3) of compound **4** formed a water-mediated hydrogen bond with Asp103 of the small domain (Table 3). The same inhibitor hydroxyl makes polar and dispersive interactions with His106 of the small domain (His106 $N_\delta1$ to phenolic hydroxyl distance of 3.4 Å) and makes a hydrogen bond with the C-terminal carboxylate of Val316. The second phenolic hydroxyl (O_4, Figure 3) forms a hydrogen bond with Glu84 of LcTS (distance of 2.9 Å, angle of 93°); the analogous residue in HTS is an alanine. The two phenolic chlorines make dispersive interactions with Thr24, Glu84, and Trp85 (Table 3). The naphthalein moiety of **4** makes van der Waals contacts with the $C_\zeta3$ and CH2 atoms of Trp85 and the $C\gamma2$ atom of Val24. The residue analogous to Trp85 in the human enzyme is an asparagine. The naphthalein ring of compound **4** also appears to interact with Glu88 (ring carbon to $O_\epsilon2$ distance of 3.3 Å), presum-

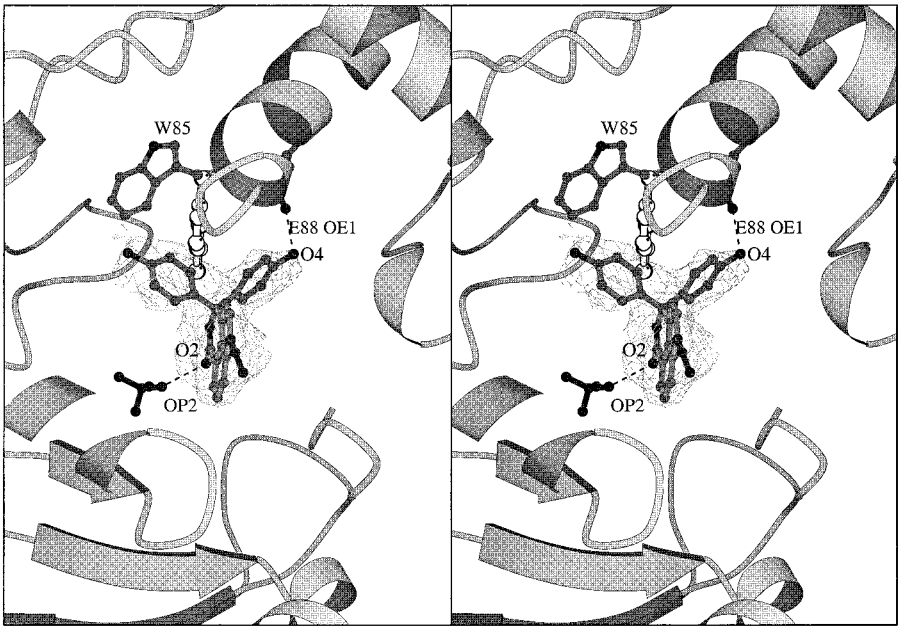

FIGURE 5: Simulated annealing omit map showing the difference electron density ($F_o - F_c$, contoured at 3σ) for compound **5** in the *L. casei* TS crystal structure. This calculation uses all of the atoms of the structure except those of the ligand and is unbiased by refinement with inclusion of the ligand molecule. This figure were prepared using the program BOBSCRIPT (R. Esnouf, 1996, unpublished).

ably through charge-quadrupole and dispersive interactions. This residue in the human structure is an arginine. Overall, the structure of the enzyme changes only slightly between the complex with phenolphthalein and that with compound **4**. The most dramatic change is in the conformation of Arg23, which formed a water-mediated hydrogen bond to the carbonyl oxygen of phenolphthalein. In the complex with **4**, Arg23 has swung away from the binding site, resuming the conformation that it occupies in the apo-TS structure.

The structure of compound **4** bound to LcTS went some way toward explaining the selectivity of that compound. The convolution of the effect of the chlorine and naphthalide derivatizations seemed to occur because both functional groups were interacting directly with residues of TS that were present in the bacterial enzyme and absent from the human enzyme (Table 3). Additionally, the chlorines may be acting indirectly to perturb the properties of the phenolic hydroxyls, which make extensive interactions with residues that differ between the two species. The interactions with the small domain may be especially important, since this region is not present in the human enzyme. When compound **4** is fit into the analogous position of a model of human TS, it appears to be poorly accommodated, physically intersecting several residues.

To address the question of how naphthalein derivatives **3** and **5** bound to the enzyme and why they lacked the specificity of compound **4**, the structure of LcTS bound to compound **5** was determined using X-ray crystallography. The structure of the complex (Figure 6) shows that, unlike compound **4**, compound **5** interacts with many of the same residues with which phenolphthalein interacted.

Although the residues defining the phenolphthalein and compound **5** sites are very similar, compound **5** binds to the site in an orientation that differs considerably from that adopted by phenolphthalein (Figure 7). In the crystal structure of the phenolphthalein−LcTS complex, three hydrogen bonds were observed involving residues Arg23, Glu60, and Asp221. In the complex with compound **5**, only the interaction with Arg23 is conserved, and this interaction is made in a different manner. A phenolic hydroxyl of compound **5** forms a hydrogen bond with atom $O_\epsilon 1$ of Glu88 (distance of 3.2 Å). A water-mediated hydrogen bond is made between Arg23 N_ϵ and the carbonyl oxygen of the naphthalide ring (Table 3). The second phenolic hydroxyl does not appear to be involved in a hydrogen bond, nor does the nitro group. Although the structure of LcTS remains broadly unchanged between the phenolphthalein and the compound **5** complex, Trp85 undergoes a large conformational change. In the complex with **5**, the side chain of Trp85 has swung away from the binding site; if it had not, compound **5** would have been excluded from this site. The compound lacks extensive interactions with residues in the small domain of LcTS.

Unlike compound **4**, compound **5** can be fit into the "humanized" *E. coli* structure without steric conflict when the two structures are overlaid. Compound **5** had few interactions with the small domain of LcTS (Table 3). Both observations are consistent with the low specificity of compound **5** for the bacterial versus the human enzyme.

The structures of the complexes between TS and compounds **4** and **5** presented two important implications. First, it appeared that the differences in species specificity between compound **4** and compound **5** arose from the different regions of the enzyme with which they interacted. As a target for species-specific enzyme inhibitors, the structures of the complexes between LcTS and compounds **4** and **5** allowed us to design and synthesize molecules with increased selectivity. Second, these complexes challenged us to understand how such apparently similar compounds bound to TS in such different manners (Figure 7). One hypothesis holds that the crystallographic structure of each complex might represent a unique, low-energy binding orientation for the ligands. Alternatively, this family of molecules might bind to LcTS in several low-energy modes, some of which were represented by the three crystal structures. We consider

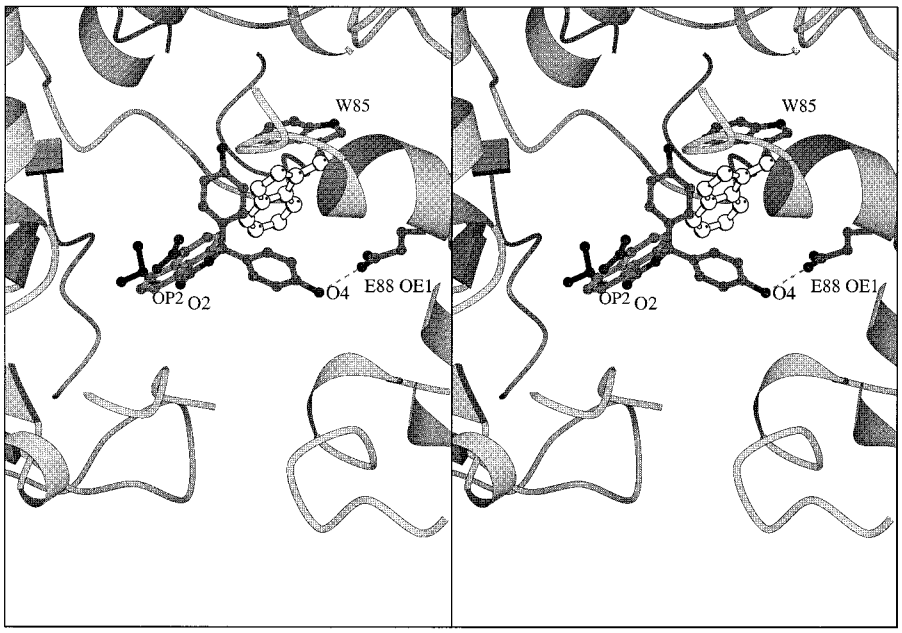

FIGURE 6: Crystal structure of compound **5** bound to TS from *L. casei*. Trp85 has reoriented by ~180° about χ_1; the orientation of this residue in the complexes with phenolphthalein and **4** is white. This figure were prepared using the program BOBSCRIPT (R. Esnouf, 1996, unpublished).

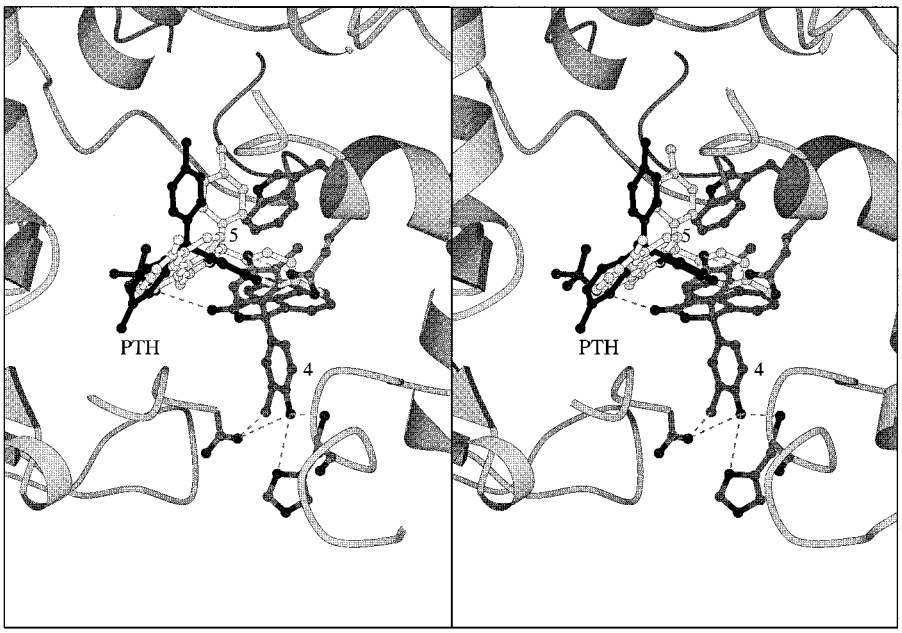

FIGURE 7: Overlay of phenolphthalein, compound **4**, and compound **5**, from their complex structures with *L. casei* TS, determined by X-ray crystallography. This figure were prepared using the program BOBSCRIPT (R. Esnouf, 1996, unpublished).

the issues of further specific design and multiple binding modes separately.

Further Species-Specific Inhibitors. The structure of the complex between compound **4** and LcTS (Figure 3) suggested there was room to add substituents to the naphthalein ring. Such substitutions should interact with residues in the small domain of LcTS, and by the same standards be less likely to inhibit HTS. Compound **7**, the 4-chloro derivative of **4**, was synthesized. This compound was a mixed competitive inhibitor of LcTS, with a K_i of 0.73 μM. It did not measurably inhibit HTS at its solubility limit (64 μM), making it more than 100-fold specific for the bacterial enzyme versus the human enzyme (Table 1).

A more dramatic departure was the deletion of one of the phenolic rings in the naphthalein series, based on our observation of the LcTS−**5** complex and the structural rearrangement of the protein induced at the binding site of one of the phenolic substituents. Most of these compounds did not inhibit LcTS significantly (unpublished results); however, the 4-nitro-3′-chloro derivative (**8**) inhibited the enzyme potently, with a K_i value of 0.25 μM. This compound showed >1000-fold specificity for LcTS over the human enzyme (Table 1). A key feature of the activity of this monophenolic derivative appears to be its derivatization on the phenolic ring by a halogen ortho to the phenolic hydroxyl; in the absence of such a substituent, activity was abolished

(data not shown). The high specificity and relative potency of this derivative make it an attractive lead for the design of further inhibitors specific for LcTS and related bacterial enzymes. These would include any that have the small domain present in LcTS, such as those occurring in the *Staphylococcus* sp. (*15*, *30*).

Multiple Binding Modes. In each of the three structures formed by TS and the phthalein analogues that we have determined, the inhibitor adopts a different binding mode in the enzyme site (Figure 7). In two structures of another TS inhibitor, sulisobenzone, the ligand was also observed to bind in two different orientations on the enzyme (*14*). Our discussions of activity thus far have assumed that the different analogues occupy different individual configurations in the binding site of TS (one compound, one configuration). It is possible that each inhibitor samples several low-energy configurations on TS. In this circumstance, the affinity of the compounds would be a product of the several different binding modes that each compound could adopt (we exclude the trivial case where the compounds adopt multiple but very similar configurations with TS).

Site-Directed Mutagenesis. Each of the three ligand−TS crystal structures shows particular contacts between the various inhibitors and the enzyme (Table 3). If the individual compounds are binding in one dominant configuration each, that represented by the crystal structure, then perturbing these interactions by site-directed mutagenesis should have a significant effect on inhibitor binding. Alternatively, if each ligand binds in several low-energy configurations, then a perturbation that is particular to a given binding mode will have less of an effect on affinity.

We tested four compounds against substitutions made at three contact residues, and one enzyme mutant where the entire small domain (residues 90−139) had been removed (*31*). In all, three mutant enzymes were tested (Table 4). The inhibitors tested included phenolphthalein and compounds **3**−**5**. The substitutions were made at Glu60 (to Asp), Trp82 (to Tyr), and Val316 (to Ala). In the various crystal structures of ligand−enzyme complexes, Glu60 appears to form a hydrogen bond with a phenolic hydroxyl of phenolphthalein (*14*). The residue does not appear to interact directly with compound **4** or **5**. Val316 appears to make dispersive interactions with phenolphthalein and compound **4**, but is too far from compound **5** to interact directly (6.2 Å is the closest contact). The C_ζ atoms of Trp82 appear to make dispersive interactions with phenolphthalein (closest distance of 4.7 Å) and make a close contact (2.5 Å) with a phenolic hydroxyl of compound **5**. Trp82 is 7.6 Å from compound **4** at its closest approach. The small domain (residues 90−139) deletion makes several polar interactions with compound **4**, as do residues close to this domain boundary, such as Glu88.

Assuming that the crystallographic configuration is the dominant binding mode, one might predict that the mutant enzyme V316A would affect the binding affinity of phenolphthalein and compound **4**, but have less of an effect on compound **5**. The extent of binding of phenolphthalein should be diminished in the mutant E60D, but the effect of the substitution should be smaller for compounds **4** and **5**. One might expect W82Y to have a small effect on compound **4** but to significantly perturb the binding of phenolphthalein.

Overall, the largest perturbations are seen with compound **4**, where substitutions at contact residues diminished the affinity by ≥10-fold. Substitution to the distant Trp82 left the affinity unperturbed. For phenolphthalein, compounds **3** and **5**, the inhibition constants with the mutant proteins did not conform to expectations based on a simple interpretation of the structures (Table 4). The mutant enzymes W82Y and E60D, both of which appear to make important contacts with phenolphthalein, have little effect on the K_i relative to the native enzyme. V316A diminishes the extent of binding of compound **5** by 13-fold, relative to that of the native enzyme, though this residue does not appear to contact the compound in the X-ray structure. Although Glu60 is observed to make a hydrogen bond with phenolphthalein, the E60D mutant has improved affinity for this inhibitor. Conversely, this substitution eliminates measurable binding by compound **3**. Though the deletion of the small domain has a 26-fold effect on the extent of binding of compound **4** (*31*), this is less than one might expect unless considerable rearrangement occurs.

The effects of these substitutions, whether on the enzyme through mutagenesis or, as with compound **8**, on the ligand, are consistent with a plastic recognition interface. This plasticity can come from protein rearrangement or ligand rearrangement or a combination of the two. Given the different binding modes adopted by the three related inhibitors in crystal structures of the complexes, our favored hypothesis is that this plasticity is at least the result of multiple low-energy binding modes being populated for several of the inhibitors.

Several investigators have observed that in a series of analogous compounds, several similar ligands can bind to the same receptor in dissimilar manners (*31*−*37*). The phenomenon is intriguing, even disturbing, because it can undermine the interpretation of affinity numbers among a series of similar compounds through structure−activity relationships (*36*). Most structure−activity relationships implicitly assume that a series of analogues will bind to a receptor in the same manner. When analogues have similar affinities but dissimilar binding modes, the basis for many structure−activity analyses breaks down.

One lesson drawn from these studies has been an emphasis on the ongoing need for experimental structure determination in ligand design efforts (*36*−*38*). It should also be noted that the observation of dissimilar binding modes for similar ligands weakens the static interpretation of even atomic resolution structures. Investigators have long recognized that ligand−protein complexes may have alternate geometries with energies close to that of the global minimum (*39*, *40*). Typically, these similar energy levels are thought to represent similar structures, but they need not. In cases where small perturbations to the ligand lead to large changes in configuration, or where multiple low-energy binding modes are available to a given ligand, interpretations of particular ligand−receptor interactions should proceed cautiously, since the structures on which they are based may represent only a partial view of the interactions that contribute to the total binding energy "landscape" of the ligand.

CONCLUSIONS

We have described the design and testing of a new series of inhibitors of thymidylate synthase that are specific for the bacterium *L. casei* versus the human enzyme. The better inhibitors bound to the bacterial enzyme at sub-micromolar

concentrations but had no measurable affinity for the human enzyme. Crystal structures of the complexes between several of these inhibitors and LcTS suggest that the specific inhibitors are interacting with a region of the bacterial enzyme that differs significantly between the bacterial and mammalian enzymes. This region borders on the substrate binding region (Figure 2) against which other TS inhibitors and drugs have been designed. The inhibitors also show selectivity in cell culture assays (*16*). These inhibitors show promise as potential lead compounds toward antimicrobial drugs that target TS.

ACKNOWLEDGMENT

We thank K. Perry and J. Finer-Moore for helpful discussions, L. Brinen for expert technical assistance, and S. Weston, B. Beadle, and R. Powers for reading the manuscript.

REFERENCES

1. Hori, T., Ayusawa, D., Shimizu, K., Koyama, H., and Seno, T. (1984) *Cancer Res. 44*, 703−709.
2. Reyes, P., and Heidelberger, C. (1965) *Mol. Pharmacol. 1*, 14−30.
3. Jones, T. R., Calvert, A. H., Jackman, A. L., Brown, S. J., Jones, J., and Harrap, K. R. (1981) *Eur. J. Cancer 17*, 11−19.
4. Santi, D. V., and Danenberg, P. V. (1984) in *Folates and Pterins* (Blakely, R. L., and Benkovic, S. J., Eds.) Vol. 1, pp 345−398, Wiley, New York.
5. Pinedo, H. M., and Peters, G. F. (1988) *J. Clin. Oncol. 6*, 1653−1664.
6. Appelt, K., Bacquet, R. J., Bartlett, C. A., Booth, C. L. J., Freer, S. T., Fuhry, M. A. M., Gehring, M. R., Herrmann, S. M., Howland, E. F., Janson, C. A., Jones, T. R., Kan, C. C., Kathardekar, V., Lewis, K. K., Marzoni, G. P., Matthews, D. A., Mohr, C., Moomaw, E. W., Morse, C. A., Oatley, S. J., Ogden, R. C., Reddy, M. R., Reich, S. H., Schoettlin, W. S., Smith, W. W., Varney, M. D., Villafranca, J. E., Ward, R. W., Webber, S., Webber, S. E., Welsh, K. M., and White, J. (1991) *J. Med. Chem. 34*, 1925−1934.
7. Jones, T. R., Varney, M. D., Webber, S. E., Lewis, K. K., Marzoni, G. P., Palmer, C. L., Kathardekar, V., Welsh, K. M., Webbe, S., Matthews, D. A., Appelt, K., Smith, W. W., Janson, C. A., Villafranca, J. E., Bacquet, R. J., Howland, E. F., Booth, C. L., Herrmann, S. M., Ward, R. W., White, J., Moomaw, E. W., Bartlett, C. A., and Morse, C. A. (1996) *J. Med. Chem. 39*, 904−917.
8. Klein, C., Chen, P., Arevalo, J. H., Stura, E. A., Marolewski, A., Warren, M. S., Benkovic, S. J., and Wilson, I. A. (1995) *J. Mol. Biol. 249*, 153−175.
9. Reich, S. H., Fuhry, M. A., Nguyen, D., Pino, M. J., Welsh, K. M., Webber, S., Janson, C. A., Jordan, S. R., Matthews, D. A., Smith, W. W., et al. (1992) *J. Med. Chem. 35*, 847−858.
10. Varney, M. D., Marzoni, G. P., Palmer, C. L., Deal, J. G., Webber, S., Welsh, K. M., Bacquet, R. J., Morse, C. A., Booth, C. L. J., Herrmann, S. M., Howland, E. F., Ward, R. W., and White, J. (1992) *J. Med. Chem. 35*, 663−676.
11. Webber, S. E., Bleckman, T. M., Attard, J., Deal, J. G., Kathardekar, V., Welsh, K. M., Webber, S., Janson, C. A., Matthews, D. A., and Smith, W. W. (1993) *J. Med. Chem. 36*, 733−746.
12. Carreras, C. W., and Santi, D. V. (1995) *Annu. Rev. Biochem. 64*, 721−762.
13. Gangjee, A., Mavandadi, F., Kisliuk, R. L., McGuire, J. J., and Queener, S. F. (1996) *J. Med. Chem. 39*, 4563−4568.
14. Shoichet, B. K., Perry, K. M., Santi, D. V., Stroud, R. M., and Kuntz, I. D. (1993) *Science 259*, 1445−1450.
15. Dale, G. E., Broger, C., Hartman, P. G., Langen, H., Page, M. G., Then, R. L., and Stuber, D. (1995) *J. Bacteriol. 177*, 2965−2970.
16. Costi, M. P., Barlocco, D., Rinaldi, M., Tondi, D., Pecorari, P., Ghelli, S., Stroud, R. M., Santi, D. V., Kuntz, I. D., Stout, T. J., Shoichet, B. K., Musiu, C., Marangiu, M. E., Pani, A., deMontis, A., Loi, A. G., and LaColla, P. (1998) *J. Med. Chem*. (submitted for publication).
17. Montfort, W. R., Perry, K. M., Fauman, E. B., Finer-Moore, J. S., Maley, G. F., Hardy, L., Maley, F., and Stroud, R. M. (1990) *Biochemistry 29*, 6964−6976.
18. Schiffer, C. A., Clifton, I. J., Davisson, V. J., Santi, D. V., and Stroud, R. M. (1995) *Biochemistry 34*, 16279−16287.
19. Climie, S., and Santi, D. V. (1990) *Proc. Natl. Acad. Sci. U.S.A. 87*, 633−637.
20. Davisson, V. J., Sirawaraporn, W., and Santi, D. V. (1989) *J. Biol. Chem. 264*, 9145−9148.
21. Davisson, V. J., Sirawaraporn, W., and Santi, D. V. (1994) *J. Biol. Chem. 269*, 30740.
22. Pogolotti, A. L., Danenberg, P. V., and Santi, D. V. (1986) *J. Med. Chem. 29*, 478−482.
23. Huang, W., and Santi, D. V. (1994) *J. Biol. Chem. 269*, 31327−31329.
24. Climie, S. C., Carreras, C. W., and Santi, D. V. (1992) *Biochemistry 31*, 6032−6038.
25. Schellenberger, U., Francis, V. S. N. K., Balaram, P., Shoichet, B. K., and Santi, D. V. (1994) *Biochemistry 33*, 5623−5629.
26. Otwinowski, Z., and Minor, W. (1997) *Methods Enzymol. 276*, 307−326.
27. Laskowski, R. A., MacArthur, M. W., Moss, D. S., and Thornton, J. M. (1993) *J. Appl. Crystallogr. 26*, 283−291.
28. Brünger, A. T. (1992) *X-PLOR Version 3.1. A System for X-ray Crystallography and NMR*, Yale University Press, New Haven, CT.
29. Segel, I. H. (1975) *Enzyme Kinetics*, Wiley, New York.
30. Finer-Moore, J., Fauman, E. B., Foster, P. G., Perry, K. M., Santi, D. V., and Stroud, R. M. (1993) *J. Mol. Biol. 232*, 1101−1116.
31. Costi, M. P., unpublished results.
32. Bolin, J. T., Filman, D. J., Matthews, D. A., Hamlin, R. C., and Kraut, J. (1982) *J. Biol. Chem. 257*, 13650−13662.
33. Badger, J., Minor, I., Kremer, M. J., Oliveira, M. A., Smith, T. J., and Griffith, J. P. (1988) *Proc. Natl. Acad. Sci. U.S.A. 85*, 3304−3308.
34. Rutenber, E., Fauman, E. B., Keenan, R. J., Fong, S., Furth, P. S., Ortiz de Montellano, P. R., Meng, E., Kuntz, I. D., DeCamp, D. L., Salto, R., Rose, J. R., Craik, C. S., and Stroud, R. M. (1993) *J. Biol. Chem. 268*, 15343−15346.
35. Weber, P. C., Pantoliano, M. W., and Thompson, L. D. (1992) *Biochemistry 31*, 9350−9354.
36. Mattos, C., Rasmussen, B., Ding, X., Petsko, G. A., and Ringe, D. (1994) *Nat. Struct. Biol. 1*, 55−58.
37. Engh, R. A., Brandstetter, H., Sucher, G., Eichinger, A., Baumann, U., Bode, W., Huber, R., Poll, T., Rudolph, R., and Saal, W. v. d. (1996) *Structure 4*, 1353−1362.
38. Hoog, S. S., Zhao, B., Winborne, E., Fisher, S., Green, D. W., DesJarlais, R. L., Newlander, K. A., Callahan, J. F., Moor, M. L., and Huffman, W. F. (1995) *J. Med. Chem. 38*, 3246−3252.
39. Hill, T. L. (1989) *Free energy transduction and biochemical cycle kinetics*, Springer-Verlag, New York.
40. Hawkes, R., Grutter, M. G., and Schellman, J. (1984) *J. Mol. Biol. 175*, 195−212.
41. Jackman, A. L., Farrugia, D. C., Gibson, W., Kimbell, R., Harrap, K. R., Stephens, T. C., Azab, M., and Boyle, F. T. (1995) *Eur. J. Cancer 31A* (7−8), 1277−1282.
42. Cunningham, D., Zalcberg, J., Smith, I., Gore, M., Pazdur, R., Burris, H., Meropol, N. J., Kennealey, G., and Seymour, L. (1996) *Ann. Oncol. 7* (2), 179−182.

BI9815896